Protein Science (1995), *4*:1998–2005. Cambridge University Press. Printed in the USA.

Crystal structure of thioltransferase at 2.2 Å resolution

SURESH K. KATTI,[1,3] ARTHUR H. ROBBINS,[1] YANFENG YANG,[2] AND WILLIAM W. WELLS[2]

[1] Bayer Corporation, Pharmaceutical Division, Institute for Chemistry, West Haven, Connecticut 06516
[2] Department of Biochemistry, Michigan State University, East Lansing, Michigan 48824

(RECEIVED May 4, 1995; ACCEPTED August 8, 1995)

Abstract

We report here the first three-dimensional structure of a mammalian thioltransferase as determined by single crystal X-ray crystallography at 2.2 Å resolution. The protein is known for its thiol-redox properties and dehydroascorbate reductase activity. Recombinant pig liver thioltransferase expressed in *Escherichia coli* was crystallized in its oxidized form by vapor diffusion technique. The structure was determined by multiple isomorphous replacement method using four heavy-atom derivatives. The protein folds into an α/β structure with a four-stranded mixed β-sheet in the core, flanked on either side by helices. The fold is similar to that found in other thiol-redox proteins, viz. *E. coli* thioredoxin and bacteriophage T4 glutaredoxin, and thus seems to be conserved in these functionally related proteins. The active site disulfide (Cys 22–Cys 25) is located on a protrusion on the molecular surface. Cys 22, which is known to have an abnormally low pK_a of 3.8, is accessible from the exterior of the molecule. Pro 70, which is in close proximity to the disulfide bridge, assumes a conserved *cis*-peptide configuration. Mutational data available on the protein are in agreement with the three-dimensional structure.

Keywords: crystal structure; dehydroascorbate reductase; disulfide; glutaredoxin; thiol oxidoreductase; thioltransferase

Thiol-disulfide oxidoreductases, which include the thioltransferase, glutaredoxin, thioredoxin family of proteins, play a vital role in maintaining the redox status of sulfhydryl groups inside the cell and thus participate in catalyzing and/or regulating a variety of cellular functions (Holmgren et al., 1986; Wells et al., 1993). They typically transfer electrons from NADPH to the substrate in reactions coupled with other specific enzymes. Thioltransferase and glutaredoxin derive their reducing equivalents from glutathione, which in turn is linked to the glutathione reductase/NADPH system, whereas thioredoxin utilizes the thioredoxin reductase/NADPH pathway for the same purpose. Thioltransferase (Askelöf et al., 1974) and glutaredoxin (Holmgren, 1976) were initially discovered due to different properties but were later found to be highly homologous in mammalian cells and in fact were shown to be one and the same protein by immunological studies (Gan & Wells, 1988). Thioredoxin, on the other hand, has similarities in function but not in the primary structure.

Thioltransferase is widely distributed in living cells. It has been isolated from a variety of sources, e.g., yeast (Nagai & Black, 1968), bovine liver (Racker, 1955; Hatakeyama et al., 1984), rat liver (Askelöf et al., 1974), pig liver (Gan & Wells, 1987a), human placenta (Larson et al., 1985), and human red blood cells (Papov et al., 1994). The protein is found to be highly conserved in its primary sequence. Pig liver thioltransferase is one of the most extensively characterized proteins in this family. It has been purified (Gan & Wells, 1986), sequenced (Gan & Wells, 1987b), cloned (Yang et al., 1989), and expressed to a high level in *Escherichia coli* (Yang & Wells, 1990). The protein (MW 12 kDa) is a single polypeptide chain of 105 residues. The N-terminus, normally found acetylated in the natural enzyme (Gan & Wells, 1987b), is free from modifications in the recombinant form. The lack of modification, however, does not seem to have a significant influence on the catalytic or the kinetic properties of the *E. coli*-expressed protein. PLTT, like other members of the thiol-disulfide oxidoreductase family, is characterized by the presence of two Cys residues separated by two other residues in its active site. It has been proposed that the two Cys residues (22 and 25) can assume dithiol or disulfide forms in a reversible fash-

Reprint requests to: Suresh K. Katti, Bayer Corporation, Institute for Chemistry, 400 Morgan Lane, West Haven, Connecticut 06516; e-mail: katti@wh.bayer.com.

[3] Affiliated with the Department of Molecular Biophysics and Biochemistry, Yale University, New Haven, Connecticut 06511.

Abbreviations: PLTT, pig liver thioltransferase; HgCl, mercuric chloride; HgO, mercuric oxide; HgAu, mercuric oxide + gold chloride; pCMBS, *p*-chloromercurybenzene sulfonate; MIR, multiple isomorphous replacement.

ion. The two states of the protein have distinguishable isoelectric points, 6.1 for the reduced form and 6.9 for the oxidized. In the recombinant protein these values shift to 6.9 and 7.9, respectively, probably due to the absence of the N-terminal blocking group (Yang & Wells, 1990). Chemical modification experiments using iodoacetamide (Gan & Wells, 1987c) have shown that Cys 22 has an abnormally low pK_a of 3.8. Many of the functionally important residues have been identified and characterized by site-directed mutagenesis experiments (Yang & Wells, 1991a). Thioltransferase catalyzes thiol-disulfide interchange among a broad range of substrates, which include small molecular weight disulfides and protein molecules (Mannervik & Axelsson, 1978). In addition to this well-known thiol-redox property, it has been shown to possess dehydroascorbate reductase activity, a function also displayed by protein disulfide isomerase in vitro (Wells et al., 1990, 1995).

We describe here the three-dimensional structure of the recombinant PLTT determined by X-ray crystallography at 2.2 Å resolution. This forms the first X-ray structure report of a mammalian protein from the thiol-oxidoreductase family of proteins. Thioredoxin from *E. coli* (Holmgren et al., 1975; Katti et al., 1990) and glutaredoxin from T4 bacteriophage (Söderberg et al., 1978; Eklund et al., 1992) have been studied by X-ray crystallography earlier. NMR structures have been reported for *E. coli* glutaredoxin, *E. coli* thioredoxin, and human thioredoxin in oxidized and reduced forms (Dyson et al., 1990; Forman-Kay et al., 1991; Sodano et al., 1991; Xia et al., 1992). Because of the high degree of sequence homology among thioltransferases, the present structure might serve as a template for the three-dimensional folds of other proteins in this entire family.

Results and discussion

Overall fold

Thioltransferase is a globular protein with approximate dimensions of 22 Å × 30 Å × 38 Å. The basic fold consists of a β-pleated sheet in the core of the molecule flanked on either side by helices (Fig. 1; Kinemage 1). On one side the helices run roughly parallel to the strands, whereas on the other side, one of the helices stretches across the sheet. The sheet, being in the center of the molecule, is largely formed of hydrophobic residues. Helices, on the other hand, show an equal distribution of hydrophobic and hydrophilic residues. Nonpolar residues make van der Waals-type contacts with those of the sheet to create two large hydrophobic cores on either side of the sheet, whereas the polar residues are distributed mostly on the exterior surface.

Table 1. *Secondary structure elements in thioltransferase*

β-Strands	β1	β2	β3	β4	
Residues	13–18	41–47	71–75	76–80	
Helices	α1	α2	α3	α4	α5
Residues	1–8	22–33	52–64	81–92	93–102

Secondary structure

Thioltransferase is a compact molecule with a large fraction of its residues (nearly 88%) belonging to well-defined secondary structural elements. The fold consists of two units, αβαβ and ββαα connected by a helix (Table 1; Kinemage 1). These secondary structural elements are linked by intervening reverse turns. Helices account for nearly 55% of the sequence and sheet for about 21%. The structure is stabilized by sequentially short-range and long-range interactions. The nonregular segments are also found to be positioned firmly in place through strong interactions often mediated by backbone atoms. These features are consistent with the known relatively high thermal stability of the protein (Gan & Wells, 1986).

The central β-sheet consists of four strands, of which three run in one direction and one in the opposite direction. The strands are mixed such that three are antiparallel (β1,β3,β4), with only the edge strand (β2) running parallel to the adjacent strand (β1) (see Fig. 5A). The pattern of the parallel (p) and the antiparallel (a) strands may be described as 2p1a3a4. The regularity in hydrogen bonding pattern is broken between β3 and β4 due to a β-bulge at residue 78. The bulge accentuates the twist in the β-sheet. β-Bulges have been observed at structurally analogous sites, between the last two consecutive antiparallel strands, in the structures of other thiol-oxidoreductases (Katti et al., 1990; Eklund et al., 1992).

Helices α1 and α3 pack on one side of the sheet. α2, α4, and α5 are on the other side. α3, which connects two nonadjacent strands, runs across the sheet. All of the helical stretches are straight and indicate no significant bending in their helical axes. α4 and α5 are contiguous in sequence but distinct in structure. A break at Gly 92 between them leads to an abrupt change in

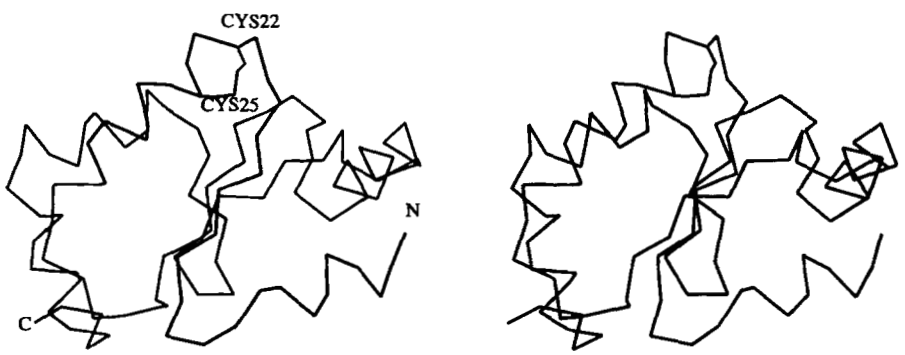

Fig. 1. Stereo view of the C^{α} backbone of thioltransferase. The N- and C-termini and active site disulfide are labeled. The active site is located on a protrusion on the surface of the protein.

direction by nearly 90°. *E. coli* thioredoxin and T4 glutaredoxin have only one C-terminal helix in place of α4–α5.

Within the helices, the hydrogen bonding pattern follows the expected geometry fairly well. Distortions, if any, occur mostly in the terminal turns. C-terminal ends often have a serine or a threonine residue, which utilizes its side-chain hydroxyl group, instead of the backbone amide, to complete the hydrogen bonding interaction with the carbonyl oxygen atom of the previous turn. In α1, the Ser 7 hydroxyl group hydrogen bonds to the carbonyl group of residue 4 (2.8 Å) instead of the backbone amide of residue 8. α2 ends with a hydrogen bond, Ser 33 OG···O residue 29 (2.8 Å). At the end of α3, Thr 64 OG1 interacts with the carbonyl oxygen of residue 60 (2.8 Å).

Thermal parameters

Figure 2 shows the distribution of thermal parameters along the polypeptide chain. The average *B*-values for the backbone atoms and all the atoms in the structure are 13.9 Å^2 and 16.9 Å^2, respectively. The entire polypeptide chain is well ordered. As might be expected the β-strands, which form the core of the molecule, exhibit the lowest *B*-values. Helices, being on the surface, display relatively higher thermal factors. Two of the highest peaks in Figure 2, at residues 21 and 51, correspond to loops exposed to the solvent. At residue 21 the polypeptide chain makes a sharp turn to form the protrusion that encompasses the active site (Kinemage 1). Both the N- and C-termini are well positioned. They, in fact, form lattice-stabilizing salt bridges in the extended crystal structure.

Active site

The active site contains two cysteine residues separated by two other residues in a sequence, Cys 22–Pro 23–Phe 24–Cys 25 (Kinemage 2). In the oxidized form, the S^γ atoms of the two Cys residues make a disulfide bridge forming a 14-membered cyclic ring. It is located in a protruding region on the surface of the protein. Residues 19–22 (Lys-Pro-Thr-Cys), just prior to the active site disulfide ring, form a reverse turn on the exterior of the molecule to create the protrusion. Cys 22 occurs at the amino-terminal end of helix α2 and is exposed to the exterior of the protein as shown in Figure 1. The sulfur atom makes a hydrogen bond with the main-chain nitrogen atom N25 (3.3 Å). These features are well conserved in thiol-oxidoreductases and may have structural significance. Cys 25, the disulfide partner, occurs almost one turn later in the interior of the molecule. Of the two cysteines, Cys 22 is known to be more reactive from alkylation experiments. Its pK_a is estimated to be as low as 3.8 (Gan & Wells, 1987c). The thiol group of this reactive cysteine is proposed to lead a nucleophilic attack on the substrates during catalysis (Yang & Wells, 1991b). The partial positive charge at the amino-terminal end of the helix (Hol, 1985) might contribute in enhancing the nucleophilicity of this thiol group. The 22SG···N25 cysteinyl hydrogen bond might also add to its reactivity by stabilizing the thiolate form. The functional Cys 22, being exposed to the exterior of the molecule, is accessible to glutathione and other substrates.

Lys 19, Arg 26, and Lys 27 are the three charged residues closest to the active site. They are displayed in a semicircle around the disulfide bond, with their C^α atoms located approximately 5.0, 6.3, and 8.3 Å away from the S–S bridge as shown in Figure 3. The charged groups on their side chains lie further out than their respective C^α atoms in the oxidized form. Of the three residues, Arg 26 has a potential to swing its side chain so as to bring its positively charged guanidinium group closer to the active site without much steric hindrance. It could thereby stabilize the anionic thiolate group of Cys 22 in the reduced form of the protein. Arg 26 may thus be critical for enhancing the reactivity of Cys 22. Site-directed mutagenesis experiments have shown that mutation of this Arg to Val greatly reduces the activity of the protein (Yang & Wells, 1991a). Negatively charged residues are distributed on the second annulus with their C^α atoms roughly 15 Å away from the active site and further out. Asp 46 is the only residue (9.2 Å) closer.

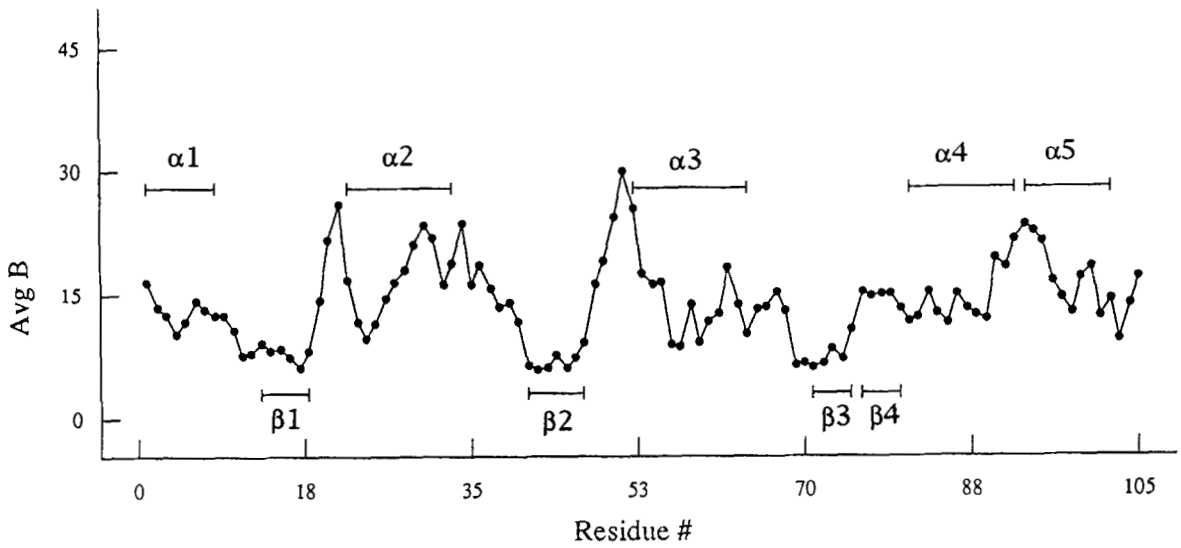

Fig. 2. Plot of the average temperature factors (Å^2) for backbone atoms against residue number.

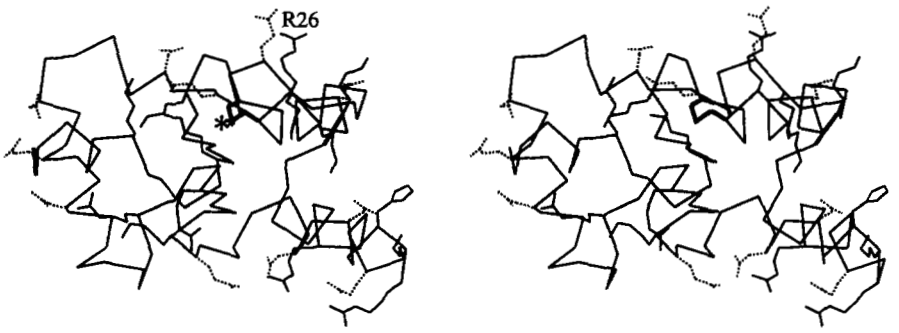

Fig. 3. Stereo view of the C^{α} backbone with the side chains of charged residues, looking down the active site disulfide bond, which is shown in thick lines (highlighted by an asterisk). Lys and Arg residues are shown in solid lines and Glu and Asp in dotted lines.

Geometry of the disulfide bridge is very similar to that found in *E. coli* thioredoxin and T-4 glutaredoxin. The side-chain torsion angles are, $\chi_1 = 168°$, $\chi_2 = -137°$ for Cys 22 and $\chi_1 = -63°$, $\chi_2 = 81°$ for Cys 25. The torsion angle about the S–S bridge is 73°. These values are very close to those observed in *E. coli* thioredoxin and T4-glutaredoxin structures. The 14-membered rings, shown superimposed in Figure 4, are geometrically very similar, but different in sequence. Thioltransferases contain a very conserved Cys-Pro-Phe/Tyr-Cys sequence. In thioredoxin and T-4 glutaredoxin, it changes to Cys-Gly-Pro-Cys and Cys-Val-Tyr-Cys, respectively. These differences may, to some extent, account for the differences in their characteristics. Mutations in this short stretch of the polypeptide have been shown to have a marked influence on the properties of thioredoxin (Krause et al., 1991) and glutaredoxin (Joelson et al., 1990) molecules.

The disulfide bridge is located in a hydrophobic environment. Ile 18, the aliphatic portion of Lys 19–Pro 20, just preceding $\alpha 2$, and Val 69–Pro 70, from the loop between $\alpha 3$ and $\beta 3$, surround the disulfide bond. The S–S bond stacks on the Pro 70 ring. Proline 70 assumes a *cis*-peptide configuration (see Fig. 7) and projects its side chain away from the backbone toward the exterior of the molecule. This *cis*-proline may have structural significance. All thiol-oxidoreductases solved so far contain a proline residue in *cis*-configuration at a structurally analogous site. The proline-76–alanine mutant of thioredoxin, which is less likely to have a *cis*-peptide at this site, was found to be less active and less stable (Kelley & Richards, 1987).

Variants of the the wild-type protein

Many of the functionally important residues have been identified through-site directed mutagenesis experiments (Yang & Wells, 1991a). Cys 22 variants were inactive, consistent with the hypothesis that it plays a central role in the electron transfer reactions mediated by this protein. Arg 26 was found to be responsible primarily for lowering the pK_a of Cys 22. As discussed above, the structure seems to support this hypothesis. Lys 27 has been implicated in stabilizing the ES intermediate. It is close to the active site and could possibly be a part of the interaction surface with the substrate. There is a second pair of cysteines, Cys 78 and Cys 82, in eukaryotic thioltransferases. Mutational analyses indicate no direct role of these two cysteines in catalysis. The structure indicates that Cys 78 is on $\beta 4$ at the bulge and Cys 82 is at the beginning of $\alpha 4$. The $S\gamma$ atoms of these two residues are more than 13 Å apart and thus cannot form a disulfide bond of relevance for catalysis. The amino-terminus is located on the surface of the protein. In the present structure, it makes an intramolecular salt bridge with Asp 52. N-acetylation, found in the wild-type natural enzyme, would interfere with the salt bridge but can be accommodated easily without any major alteration in the structure.

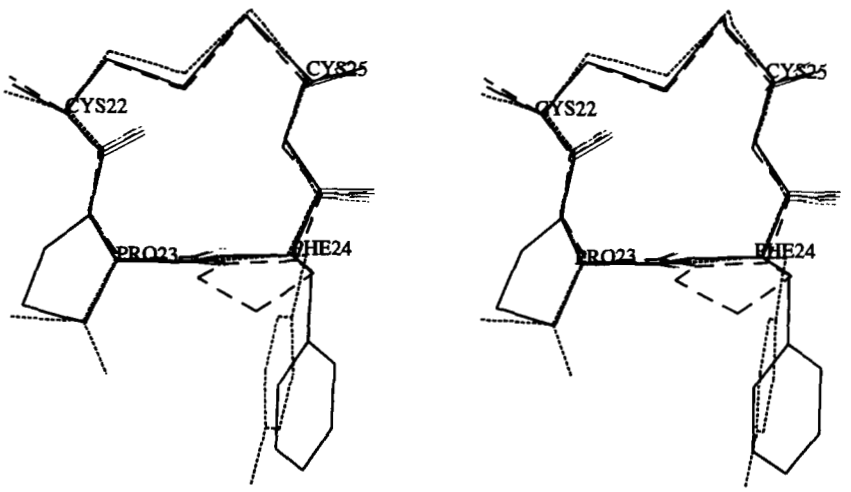

Fig. 4. Stereo view of the 14-membered ring formed by the disulfide bond in thioltransferase (Cys-Pro-Phe-Cys in solid lines) shown superimposed on that from *E. coli* thioredoxin (2TRX, Cys-Gly-Pro-Cys in dashed lines) and T4-glutaredoxin (1AAZ, Cys-Val-Tyr-Cys in dotted lines). Numbering refers to the PLTT sequence.

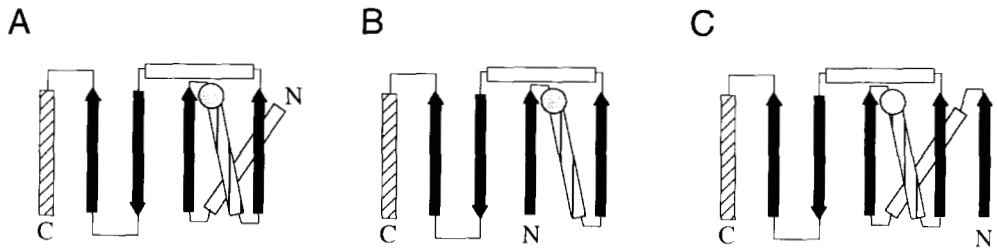

Fig. 5. Schematic representation of the folding of (**A**) thioltransferase, (**B**) T4 glutaredoxin, and (**C**) *E. coli* thioredoxin. β-Strands are shown as thick arrows and helices as rectangular boxes. Striped helices are on the front side of the sheet and open ones on the other side. Location of the active site is highlighted with a circle.

Comparison among thioltransferases

Alignment of the primary structures of mammalian thioltransferases shows a high degree of sequence identity, exceeding 80% (Wells et al., 1993). Even among the changes, most are found to be conservative substitutions. In our model, all of the changes map to the surface of the protein. The core and the overall fold are completely retained. Thus, the present structure may be used as a template for the structures of all of the proteins in the thioltransferase family.

Comparison with other thiol-oxidoreductases

The overall fold of thioltransferase is very similar to that of *E. coli* thioredoxin and T4 bacteriophage glutaredoxin. They essentially contain a mixed β-sheet in the core packed on either side by helices. *E. coli* thioredoxin, which is 108 residues long, has an additional β-strand tagged on at the N-terminal end. Glutaredoxin, which contains only 87 residues, starts with β1 without the first helix, as shown schematically in Figure 5. The fold seems to be characteristic of these functionally related proteins. Even in larger proteins, like bacterial DsbA and glutathione-*S*-transferase, domains that mediate thiol–redox functions retain the same fold (Reinemer et al., 1991; Ji et al., 1992; Martin et al., 1993).

Even though the overall fold is similar in thioltransferase, thioredoxin and glutaredoxin molecules, there are distinct differences in the relative orientations of their secondary structural elements in three dimensions. When these molecules are viewed from a similar direction with respect to the active site disulfide (Fig. 6), major differences are observed on the α1/α3 face of the molecule. α1 in thioltransferase is packed more or less on the middle of the β-sheet. It makes contacts with residues on the central two strands. In thioredoxin, the analogous helix is shifted laterally toward one end of the sheet due to its link with the additional N-terminal strand. This helix is missing altogether in the T4-glutaredoxin structure. Helix corresponding to α3, which connects two nonadjacent strands of the mixed β-sheet, varies in length but is oriented spatially in a somewhat similar fashion. The common four strands of the β-sheet and the helix α2 show more striking similarities in their relative orientations. The C-terminal helix in glutaredoxin is oriented close to α4, and in thioredoxin it is somewhat similar to α5. Thioltransferase contains both.

The region close to the active site in thioltransferase is flat and devoid of any pronounced clefts like in the thioredoxin structure. In this respect, it is distinctly different from T4 glutaredoxin, which has been described as having a cleft-like active site pocket created by surrounding loops (Eklund et al., 1992). Even though the disulfide conformation is very similar in the three molecules, the architecture of the neighboring region, especially close to the α3 helix, is very different due to the varying lengths of this helix in the three proteins. Consequently, the segment linking α3 to the ββαα motif is seen to span spatially different regions with respect to the molecule. These three proteins, though functionally related, are known to interact with different effector macromolecules in the cell. Differences in their three-dimensional structures observed here might contribute in conferring such specificities.

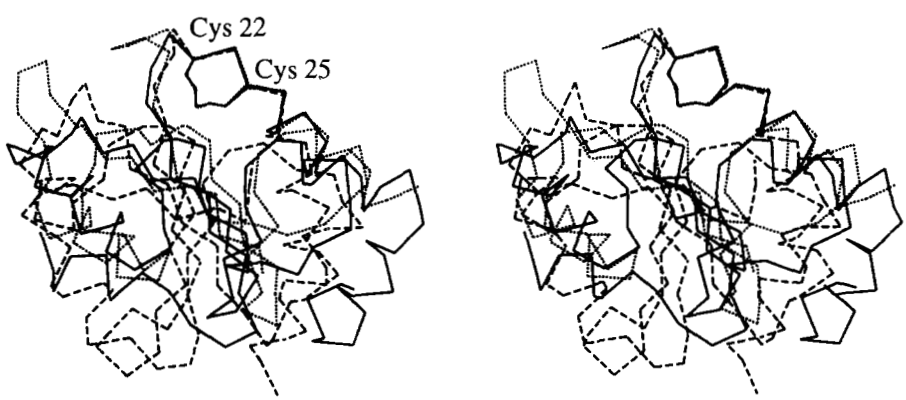

Fig. 6. C^{α} backbone traces of thioltransferase (solid lines), *E. coli*, thioredoxin (2TRX, dashed lines) and T4-glutaredoxin (1AAZ, dotted lines) viewed from a similar direction with respect to the active site disulfide (labels refer to PLTT). α1/α3 face of the protein is on the left side.

Materials and methods

Crystallization

Recombinant PLTT was purified according to the procedure described by Yang and Wells (1990). The enzyme, usually stored at −70 °C in 25 mM phosphate, pH 6.5, 25% glycerol, was thawed and treated with 10 mM hydroxyethyl disulfide at room temperature for 30 min to convert it to the oxidized form. The sample was dialyzed against 10 mM sodium phosphate buffer at pH 6.5 to remove excess reagents and then concentrated to 10 mg/mL using Centricon 3 tubes (3,000 MW cutoff). The protein was homogeneous by SDS gels. It was crystallized by vapor diffusion in a hanging drop setup. Five microliters of the protein sample was mixed with 5 μL of the reservoir solution containing 60% saturated ammonium sulfate, 100 mM acetate buffer at pH 5.5, and then equilibrated against the reservoir at 4 °C. Rectangular plate-like crystals grew in clusters over a week and were large enough (0.2 × 0.2 × 0.02 mm) for X-ray diffraction experiments. Typically, the crystalline clusters had to be cut to separate a single crystal, as judged by extinction properties under polarized light, before mounting for X-ray analysis. The crystals were stored in an artificial mother liquor containing 100 mM acetate buffer at pH 5.5 with 70% saturated ammonium sulfate solution.

Data collection

Single crystals, mounted inside sealed glass capillaries along with a droplet of the synthetic mother liquor, showed X-ray diffraction patterns extending to beyond 2.2 Å resolution. The crystals were characterized using 25 well-centered reflections collected on a Rigaku AFC-5R diffractometer with CuKα radiation from a Rigaku RU300 rotating anode source. They belong to the monoclinic system, space group $P2_1$, with $a = 23.4$, $b = 64.4$, $c = 29.5$ Å, and $\beta = 91.1°$. The unit cell contains two protein molecules and 35% solvent with $V_m = 1.87$ Å^3/Da, which is close to the lower end of the range of values observed for proteins (Matthews, 1968). Three-dimensional X-ray diffraction data were collected at room temperature using a multiwire SDMS dual area detector system in 0.1° ω frames, counting each frame for 30 s (Xuong et al., 1978). The crystals were stable under X-ray irradiation for at least 2–3 days, long enough to collect the entire data set from one single crystal. The data were integrated and processed using the software package provided by SDMS (Howard et al., 1985). Data sets from the derivative crystals were complete to 2.8 Å resolution with R_{merge} in the range 4.4–6.2%. The native data set contains a total of 4,467 unique reflections extending to 2.2 Å resolution (99% complete) with $R_{merge} = 5.6\%$.

Structure determination

The structure was solved by the MIR method using four different heavy-atom derivatives: (1) HgCl; (2) HgO; (3) HgAu double derivative; and (4) pCMBS. The derivatives were prepared by soaking native crystals in synthetic mother liquor containing the respective heavy-atom reagents at 1 mM concentration. The double derivative was obtained by soaking gold chloride-derivatized crystals in HgCl solution according to the same procedure. The pCMBS derivative had one single mercury site, whereas the rest indicated heavy atom substitutions at multiple locations. Phases obtained from the pCMBS derivative were used to identify heavy atom sites in the other three by cross difference Fourier calculations. These positions matched the solutions obtained independently by interpreting the difference Patterson maps as well as by vector search procedure using the program HASSP (Terwilliger et al., 1987). Heavy-atom derivative statistics are summarized in Table 2.

Heavy-atom parameters were refined by a least-squares procedure to minimize lack of closure errors using the PROTEIN package (Steigemann, 1992). Anomalous dispersion data were included during phase calculation. The overall mean figure of merit converged to 0.88 for data up to 3.0 Å resolution. Electron density maps calculated at this stage were partially interpretable. Three of the four strands in the β-sheet and parts of helices could be traced. Phases computed from the partial model consisting of 76 residues built as "polyalanine" were combined with the MIR phases with equal weighting. The combined mean figure of merit increased to 0.89 and the maps revealed 91 residues with recognizable sequence. The phase combination procedure was repeated in two more rounds, using increasingly

Table 2. *Heavy-atom derivative data statistics*

	Native	pCMBS	HgCl	HgO	HgAu
Soak duration (h)		12	12	96	12+12
Concentration (mM)		1	1	1	1+1
Total reflections	21,047	10,617	23,591	16,372	10,951
Unique data	2,199	2,084	2,167	2,165	2,179
Complete to 2.8Å	99.6%	96.1%	99.4%	99.3%	99.5%
R-merge[a]	0.045	0.05	0.044	0.062	0.057
R-isomorphous[b]		0.14	0.16	0.18	0.13
No. of sites		1	2	4	2
R-cullis[c]		0.77	0.57	0.36	0.57
Phasing power[d]		1.15	1.98	3.53	1.97

[a] R-merge $= \Sigma_h \Sigma_i |I(h)_i - \langle I(h) \rangle| / \Sigma_h \Sigma_i I(h)$.
[b] R-isomorphous $= \Sigma_h |I(\text{deri}) - I(\text{nati})| / \Sigma_h I(\text{nati})$.
[c] R-cullis $= \Sigma \| FPH_{obs}| \pm |FP_{obs}\| - |FH_{cal}\| / \Sigma \| FPH_{obs}| \pm |FP_{obs}\|$.
[d] Phasing power $= f_H$/RMS lack of closure error.

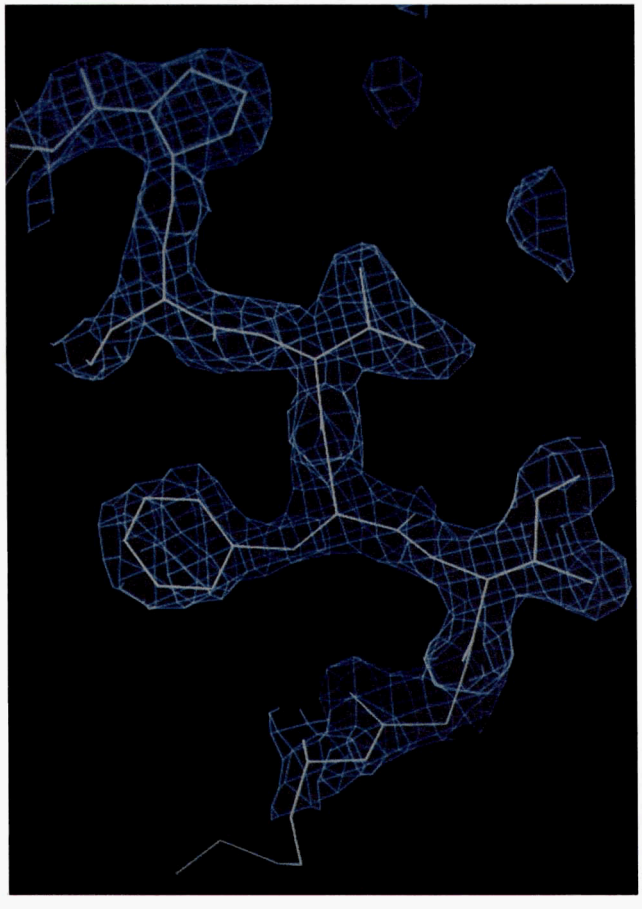

Fig. 7. A section of the final $2F_o - F_c$ electron density map with calculated phases at 2.2 Å resolution shown superimposed on Pro 70–Arg 71–Val 72–Phe 73–Ile 74–Gly 75 of the protein model. The contours are drawn at the 1.5σ level. Arg side chain is clipped in the Z-direction. Pro 70 has a *cis*-peptide configuration.

larger portions of the interpreted protein model (91 and 101 residues). The maps generated at this stage (figure of merit = 0.92) indicated very clearly the complete trace of the polypeptide chain and the side-chain orientations.

The amino acid sequence fits the electron density maps unambiguously as shown in Figure 7. The protein model was built on an ESV work station using FRODO (Jones, 1978). The protein molecules pack in the unit cell without making any unacceptable contacts with the symmetry-related molecules.

Refinement

The structure has been refined using data between 8 and 2.2 Å resolution by a simulated annealing procedure followed by positional refinement in the program package X-PLOR (Brünger, 1992). The resolution was extended stepwise by adding data in shells of $(\sin\theta/\lambda)$. The atomic temperature factors were held fixed at 18 Å^2 during the initial stages. The model was rebuilt over the course of the refinement using $(2F_o - F_c)$ and omit maps. The individual isotropic B-factor refinement was initiated at 2.4 Å resolution ($R = 0.24$) setting the target B-factor deviation for bonded atoms in the backbone and the side chains to

Table 3. *Refinement statistics*

Resolution (Å)	8–2.2
Number of unique reflections	4,369
R-factor	0.189
R-free	0.264
Non-hydrogen atoms of protein	818
Water molecules	67
Average B-factors (Å^2)	
Backbone	13.9
All atoms	16.9
RMS bond length deviation (Å)	0.012
RMS bond angle deviation (°)	2.7
RMS ΔB for bonded atoms (Å^2)	3.3

1.5 Å^2 and 2.0 Å^2, respectively. Water molecules were picked from peaks larger than 3σ in the difference Fourier maps using the program SOLVENT (Katti et al., 1990) to make sensible hydrogen bonding interactions. Water molecules that refined with individual Bs greater than 60 Å^2 were omitted. The procedure was repeated until no additional waters were picked. The R-value for the final model, consisting of 105 amino acid residues and 67 water molecules, with acceptable stereochemistry (σ-bond = 0.012 Å, σ– bond angle = 2.7°) is 0.189 for all data between 8 and 2.2 Å resolution. The R-free calculated for 10% of the test data set not included in refinement is 0.264. The refinement statistics are summarized in Table 3. The coordinates have been deposited in the Brookhaven Protein Data Bank. The Ramachandran plot shown in Figure 8 indicates that the backbone conformation lies well within the allowed region.

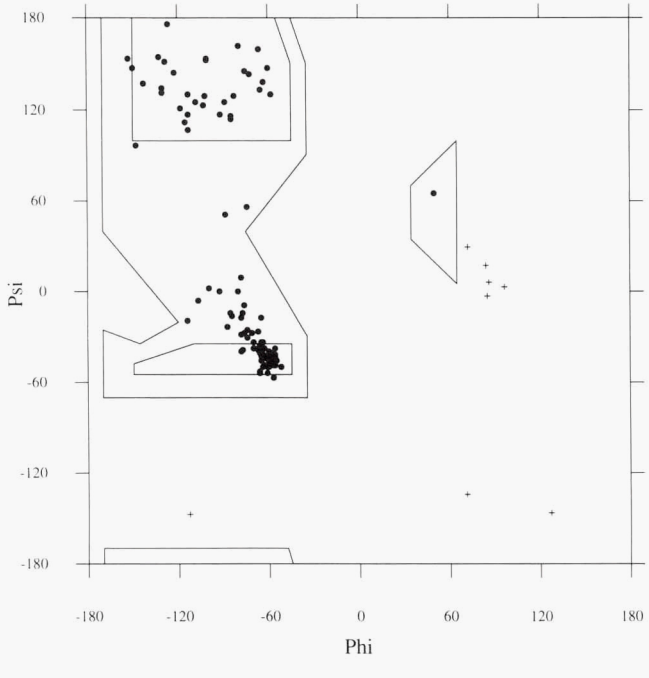

Fig. 8. Ramachandran plot for the main-chain torsion angles (ϕ, ψ). Glycine residues are marked as +.

Acknowledgments

We thank Drs. Sookhee Ha, David Hartsough, Paul Blake, and Tenna Sakai for helpful discussions, and Dr. Robert Tilton for valuable suggestions and encouragement throughout the course of this investigation. The protein preparation part of the work carried out at the Michigan State University was supported by research grant DK-44456 and CA-51972 to W.W.W. from the National Institutes of Health.

References

Askelöf P, Axelsson K, Eriksson SA, Mannervik B. 1974. Mechanism of action of enzymes catalyzing thiol–disulfide interchange—Thioltransferase rather than transhydrogenases. *FEBS Lett 38*:263–267.

Brünger AT. 1992. *X-PLOR version 3.1: A system for crystallography and NMR. Reference manual.* New Haven, Connecticut: Yale University.

Dyson HJ, Gippert GP, Case DA, Holmgren A, Wright PE. 1990. Three-dimensional solution structure of the reduced form of *Escherichia coli* thioredoxin determined by nuclear magnetic resonance spectroscopy. *Biochemistry 29*:4129–4136.

Eklund H, Ingelman M, Söderberg BO, Uhlin T, Nordland P, Nikkola M, Sonnerstam U, Joelson T, Petratos K. 1992. Structure of oxidized bacteriophage T4 glutaredoxin (thioredoxin). *J Mol Biol 228*:596–618.

Forman-Kay JD, Clore GM, Wingfield PT, Gronenborn AM. 1991. High-resolution three-dimensional structure of reduced recombinant human thioredoxin in solution. *Biochemistry 30*:2685–2698.

Gan ZR, Wells WW. 1986. Purification and properties of thioltransferase. *J Biol Chem 261*:996–1001.

Gan ZR, Wells WW. 1987a. Preparation of homogeneous pig liver thioltransferase by a thiol:disulfide mediated pI shift. *Anal Biochem 162*:265–273.

Gan ZR, Wells WW. 1987b. The primary structure of pig liver thioltransferase. *J Biol Chem 262*:6699–6703.

Gan ZR, Wells WW. 1987c. Identification and reactivity of the catalytic site of pig liver thioltransferase. *J Biol Chem 262*:6704–6707.

Gan ZR, Wells WW. 1988. Immunological characterization of thioltransferase from pig liver. *J Biol Chem 263*:9050–9054.

Hatakeyama M, Tonimoto Y, Mizoguchi T. 1984. Purification and some properties of bovine liver cytosol thioltransferase. *J Biochem (Tokyo) 95*:1811–1818.

Hol WGJ. 1985. The role of the alpha-helix dipole in protein function and structure. *Prog Biophys Mol Biol 45* :149–195.

Holmgren A. 1976. Hydrogen donor system for *E. coli*. ribonucleotide diphosphate reductase dependent upon glutathione. *Proc Natl Acad Sci USA 73*:2275–2279.

Holmgren A, Brändén CI, Jörnvall H, Sjöberg BM. 1986. In: *Thioredoxin and glutaredoxin systems—Structure and function.* New York: Raven Press.

Holmgren A, Söderberg BO, Eklund H, Brändén CI. 1975. Three-dimensional structure of *E. coli* thioredoxin-S_2 to 2.8 Å resolution. *Proc Natl Acad Sci USA 72*:2305–2309.

Howard AJ, Nielsen C, Xuong NH. 1985. Software for a diffractometer with multiwire area detector. *Methods Enzymol 114*:452–472.

Ji X, Zhang P, Armstrong RN, Gilliland GL. 1992. The three-dimensional structure of a glutathione-*S*-transferase from the Mu gene class. Structural analysis of the binary complex of isozyme 3-3 and glutathione at 2.2 Å resolution. *Biochemistry 31*:10169–10184.

Joelson T, Sjöberg BM, Eklund H. 1990. Modifications of the active center of T4 thioredoxin by site-directed mutagenesis. *J Biol Chem 265*: 3183–3188.

Jones TA. 1978. A graphics model building and refinement system for macromolecules. *J Appl Crystallogr 11*:268–272.

Katti SK, LeMaster DM, Eklund H. 1990. Crystal structure of thioredoxin from *Escherichia coli* at 1.68 Å resolution. *J Mol Biol 212*:167–184.

Kelley RF, Richards FM. 1987. Replacement of proline-76 with alanine eliminates the slowest kinetic phase in thioredoxin folding. *Biochemistry 26*:6765–6774.

Krause G, Lundström J, Barea JL, de la Cuesta CP, Holmgren A. 1991. Mimicking the active site of protein disulfide isomerase by substitution of proline 34 in *Escherichia coli* thioredoxin. *J Biol Chem 266*:9494–9500.

Larson K, Eriksson V, Mannervik B. 1985. Thioltransferase from human placenta. *Methods Enzymol 113*:520–524.

Mannervik B, Axelsson K. 1978. The roles of glutathione, thioltransferase and glutathione reductase in the scission of sulfur–sulfur bonds. In: Sies H, Wenden A, eds. *Function of glutathione in liver and kidney.* New York: Springer-Verlag. pp 148–153.

Martin JL, Bardwell JCA, Kuriyan J. 1993. Crystal structure of the DsbA protein required for disulfide bond formation in vivo. *Nature (Lond) 365*:464–468.

Matthews BW. 1968. Solvent content of protein crystals. *J Mol Biol 33*:491–497.

Nagai S, Black S. 1968. A thiol-disulfide *trans*-hydrogenase from yeast. *J Biol Chem 243*:1942–1947.

Papov VV, Gravina SA, Mieyal JJ, Biemann K. 1994. The primary structure and properties of thioltransferase (glutaredoxin) from human red blood cells. *Protein Sci 3*:428–434.

Racker E. 1955. Glutathione-homocystine transhydrogenase. *J Biol Chem 217*:867–874.

Reinemer P, Dirr HW, Landenstein R, Schäffer J, Gallay O, Huber R. 1991. The three-dimensional structure of class π glutathione-*S*-transferase in complex with glutathione sulfonate at 2.3 Å resolution. *EMBO J 10*:1997–2005.

Sodano P, Xia TH, Bushweller JH, Björnberg O, Holmgren A, Billeter M, Wüthrich K. 1991. Sequence specific ^{1}H n.m.r. assignments and determination of the three-dimensional structure of reduced *Escherichia coli* glutaredoxin. *J Mol Biol 221*:1311–1324.

Söderberg BO, Sjöberg BM, Sonnerstam U, Brändén CI. 1978. Three-dimensional structure of thioredoxin induced by bacteriophage T4. *Proc Natl Acad Sci USA 75*:5827–5830.

Steigemann W. 1992. *PROTEIN: A program system for the crystal structure analysis of proteins. version 3.1. User's guide.* Max-Planck-Institüt für Biochemie.

Terwilliger TC, Kim SH, Eisenberg D. 1987. Generalized method of determining heavy-atom positions using the difference Patterson function. *Acta Crystallogr A 43*:1–5.

Wells WW, Xu DP, Washburn MP. 1995. Glutathione:dehydroascorbate oxido reductases (EC 1.8.5.1). *Methods Enzymol 252*:30–38.

Wells WW, Xu DP, Yang Y, Rocque PA. 1990. Mammalian thioltransferase (glutaredoxin) and protein disulfide isomerase have dehydroascorbate reductase activity. *J Biol Chem 265*:15361–15364.

Wells WW, Yang Y, Deits TL, Gan ZR. 1993. Thioltransferases. *Adv Enzymol 66*:149–201.

Xia TH, Bushweller JH, Sodano P, Billeter M, Björnberg O, Holmgren A, Wüthrich K. 1992. NMR structure of oxidized *Escherichia coli* glutaredoxin: Comparison with reduced *E. coli* glutaredoxin and functionally related proteins. *Protein Sci 1*:310–321.

Xuong NH, Freer ST, Hamlin R, Nielsen C, Vernon W. 1978. The electronic stationary picture method for high-speed measurement of reflection intensities from crystals with large unit cells. *Acta Crystallogr A 34*: 289–296.

Yang Y, Gan ZR, Wells WW. 1989. Cloning and sequencing of the cDNA encoding pig liver thioltransferase. *Gene 83*:339–346.

Yang Y, Wells WW. 1990. High-level expression of pig liver thioltransferase (glutaredoxin) in *Escherichia coli*. *J Biol Chem 265*:589–593.

Yang Y, Wells WW. 1991a. Identification and characterization of the functional amino acids at the active center of pig liver thioltransferase by site-directed mutagenesis. *J Biol Chem 266*:12759–12763.

Yang Y, Wells WW. 1991b. Catalytic mechanism of thioltransferase. *J Biol Chem 266*:12766–12771.